

Supplementary Information

**One-dimensional porous carbon-supported Ni/Mo₂C dual catalyst for
efficient water splitting****

*Zi-You Yu, Yu Duan, Min-Rui Gao, Chao-Chao Lang, Ya-Rong Zheng, and Shu-Hong Yu**

*Division of Nanomaterials and Chemistry, Hefei National Laboratory for Physical Sciences at
Microscale, Collaborative Innovation Center of Suzhou Nano Science and Technology, Department of
Chemistry, CAS Center for Excellence in Nanoscience, Hefei Science Center of CAS, University of
Science and Technology of China, Hefei 230026, China.*

**Corresponding author. E-mail: shyu@ustc.edu.cn (S.H.Y.)*

Experimental section

Preparation of NiMoO₄ nanorods. The NiMoO₄ nanorods were prepared by a hydrothermal method modified in our previous work.¹ Briefly, 2 mmol Ni(NO₃)₂·6H₂O and 2 mmol Na₂MoO₄·2H₂O were dissolved in 35 mL H₂O. The clear solution was transferred into a 50 mL Teflon-lined stainless autoclave and kept at 150 °C for 6 h. After reaction, the solution was centrifuged, washed, and dried to obtain NiMoO₄ nanorods.

Preparation of Ni/Mo₂C-PC catalyst. The NiMoO₄ nanorods (40 mg) were dispersed into 100 mL Tris buffer aqueous solution (2 mg mL⁻¹, pH 8.5) and then 60 mg dopamine hydrochloride was added under magnetic stirring. The reaction was stirred continuously at room temperature for 24 h to form the uniform polydopamine (PDA) coating. The NiMoO₄@PDA nanorods can be obtained by centrifugation and washed with deionized water. The dried solid was treated at 800 °C for 2 h with a heating rate of 2 °C min⁻¹ under Ar atmosphere to get the final Ni/Mo₂C-PC catalyst. The Ni and Mo₂C contents in the Ni/Mo₂C-PC catalyst were 20.9 wt% and 29.7 wt%, respectively, calculated from the ICP result. For comparison, the catalysts treated at 500, 600, 700, and 900 °C were prepared (Figure S2). Meanwhile, the catalysts with 0, 10, 20, 40, and 80 mg dopamine hydrochloride added were also prepared under other conditions unchanged (Figure S3).

Preparation of Mo₂C-PC, Ni-PC, and PC catalysts. At first, we tried to obtain Mo₂C-PC by dissolving the Ni from Ni/Mo₂C-PC sample treated in the acidic solution, because Mo₂C is stable in diluted acidic solution while Ni is not. However, even in 0.1 M HCl solution without heating, most of nanoparticles were removed and the XRD spectrum mainly contains the peaks of carbon (Figure S4). The same result was repeated several times. Based on the elemental mapping images, most of large Ni nanoparticles are surrounded by the small Mo₂C nanoparticles. It may be due to the small Mo₂C nanoparticle escaped from porous carbon after dissolving the large Ni nanoparticle support. Therefore, Mo₂C-PC was prepared by using MoO₃ as the Mo source and polypyrrole as the carbon source, because MoO₃ was dissolved quickly in the alkaline polymerization of dopamine. Firstly, we prepared MoO₃ nanorods according to the previously reported method.² Then 80 mg MoO₃ nanorods and 0.1 mL pyrrole were dispersed into 60 mL HCl solution (1 M). 0.5 g ammonium persulphate was dissolved in 20 mL H₂O and was added the above solution dropwise under magnetic stirring. After 12 hours, the product was centrifuged and washed. Finally, Mo₂C-PC was obtained by thermal annealing

at 800 °C for 2 h with 2 °C min⁻¹ under Ar atmosphere (Figure S5). The content of Mo₂C in the Mo₂C-PC catalyst was 52.7 wt% from the ICP result.

Ni-PC was prepared with the same synthesis method of Ni/Mo₂C-PC except using the Ni-based precursor replacing the NiMoO₄ nanorod (Figure S5). Ni-based precursor (NiC₂O₄ nanorod) was synthesized based on a previous work.³ Tuning the initial mass of Ni-based precursor (about 46 mg) led to about 47.6 wt% Ni content in Ni-PC catalyst from ICP result.

PC was prepared by treating Ni/Mo₂C-PC in concentrated HNO₃ at 60 °C for 5 hours (Figure S4). The sum content of Ni and Mo₂C in PC was lower than 1 wt% from ICP result.

Characterizations. SEM images of surface morphology were obtained from a Zeiss Supra 40 SEM operating at 5 kV. TEM images were carried out a Hitachi H7650 TEM operating at 120 kV. HRTEM images and element mappings were obtained on an Atomic Resolution Analytical Microscope (JEM-ARM 200F) operating at 200 kV. Raman spectrum was recorded on a Renishaw System 2000 spectrometer with an excitation wavelength of 514.5 nm. X-ray photoelectron spectroscopy (XPS) was collected on an ESCALab MKII X-ray photoelectron spectrometer with an X-ray source (Mg K α $h\nu$ = 1253.6 eV). Crystalline structure was analyzed by the powder X-ray diffraction (XRD) with a Philips X'Pert Pro Super X-ray diffractometer equipped using Cu K α radiation at a wavelength of 1.541841 Å. N₂ sorption analysis at 77 K was determined with an ASAP 2020 (Micromeritics, USA). The Ni and Mo contents of catalysts were measured by inductively coupled plasma mass spectrometry (Thermo Scientific PlasmaQuad 3) after dissolving the samples with hot concentrated HNO₃.

Electrocatalytic study. Electrochemical measurements for HER and OER were carried out in a three-electrode configuration with IM6ex electrochemical workstation (ZAHNER elektrik, Germany). A rotating disk electrode made of glassy carbon (GC, 5 mm diameter, 0.196 cm²) electrode with catalyst was used as the working electrode. Graphite rod and saturated calomel electrode (SCE) were used as the counter and reference electrodes, respectively. The potential difference between SCE and RHE was calibrated based on the cyclic voltammetry test in H₂-saturated 1.0 M KOH electrolyte at a scan rate of 1 mV s⁻¹. E(RHE) = E(SCE) + 1.064 V. The catalyst ink was prepared by mixing 5 mg catalysts with 960 μ L ethanol and 40 μ L Nafion solution (5 wt%) under sonication. Then, 20 μ L of the catalyst ink was transferred onto the GC electrode with a catalyst loading of about 0.50 mg cm⁻². Commercial Pt/C (20 wt%, Johnson Matthey) was tested with a catalyst loading of 0.25 mg cm⁻² for comparison. Before the electrochemical tests, the electrolyte (1 M KOH) was bubbled with nitrogen gas for HER and

oxygen gas for OER. The polarization curves were obtained from the linear sweep voltammetry with a scan rate of 5 mV s^{-1} and a rotation rate of 1,600 r.p.m. It should be noted that we defined the potential at a HER or OER current density of 1 mA cm^{-2} as the onset potential.⁴

The catalyst was supported on Ni foam with a mass loading of 2.0 mg cm^{-2} for HER and OER stability tests in a three-electrode configuration. The catalyst Ni/Mo₂C-PC loaded on Ni foam was used as both cathode and anode in a two-electrode configuration for overall water splitting. The LSV curves were obtained at a scan rate of 2 mV s^{-1} and chronoamperometry experiments were conducted at applied bias voltage of 1.74 V for 10 h. All data were iR-corrected unless otherwise specified.

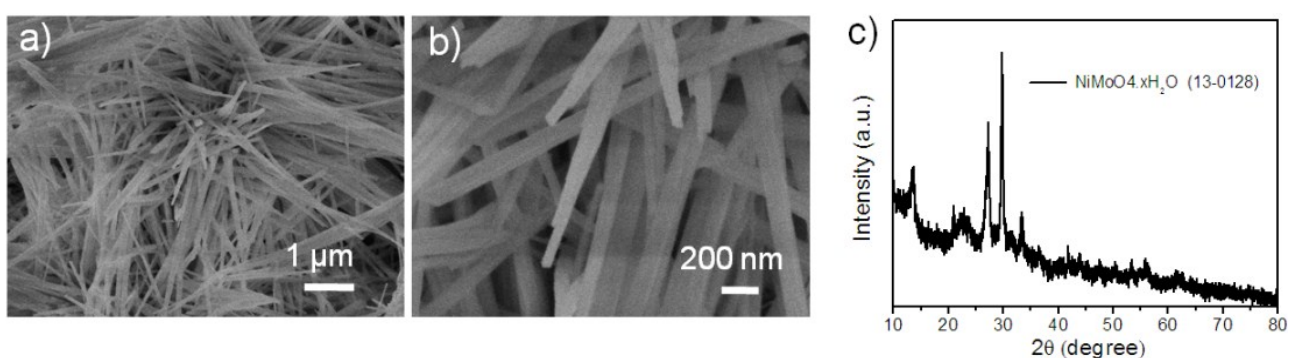


Fig. S1 (a-b) SEM images and (c) XRD pattern of NiMoO₄ nanorods.

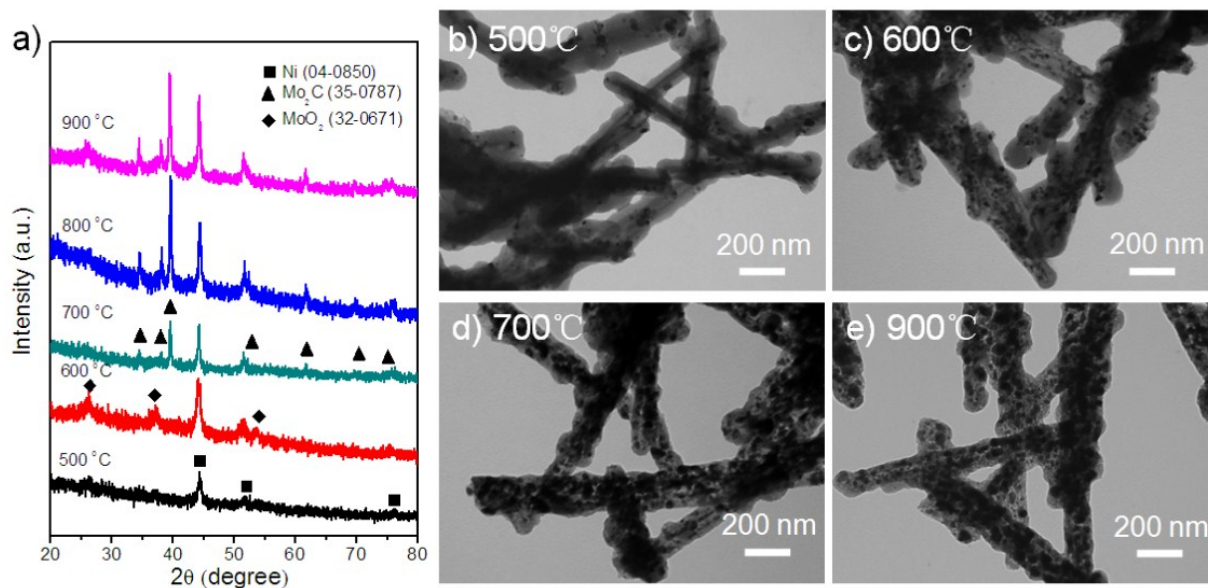


Fig. S2 (a) XRD patterns of NiMoO₄@PDA samples treated at 500-900 °C. TEM images of NiMoO₄@PDA treated at (b) 500 °C, (c) 600 °C, (d) 700 °C, and (e) 900 °C. Condition: keeping the masses of NiMoO₄ and dopamine constant (40 mg NiMoO₄ and 60 mg dopamine).

Note: The XRD patterns of samples treated at 500-600 °C can be indexed to Ni and MoO₂ phase. After increasing the temperature to 700-900 °C, the XRD peaks can be indexed to Ni and Mo₂C phase. Therefore, the annealing process can be reasonably speculated through the following reaction with the increased annealing temperature:



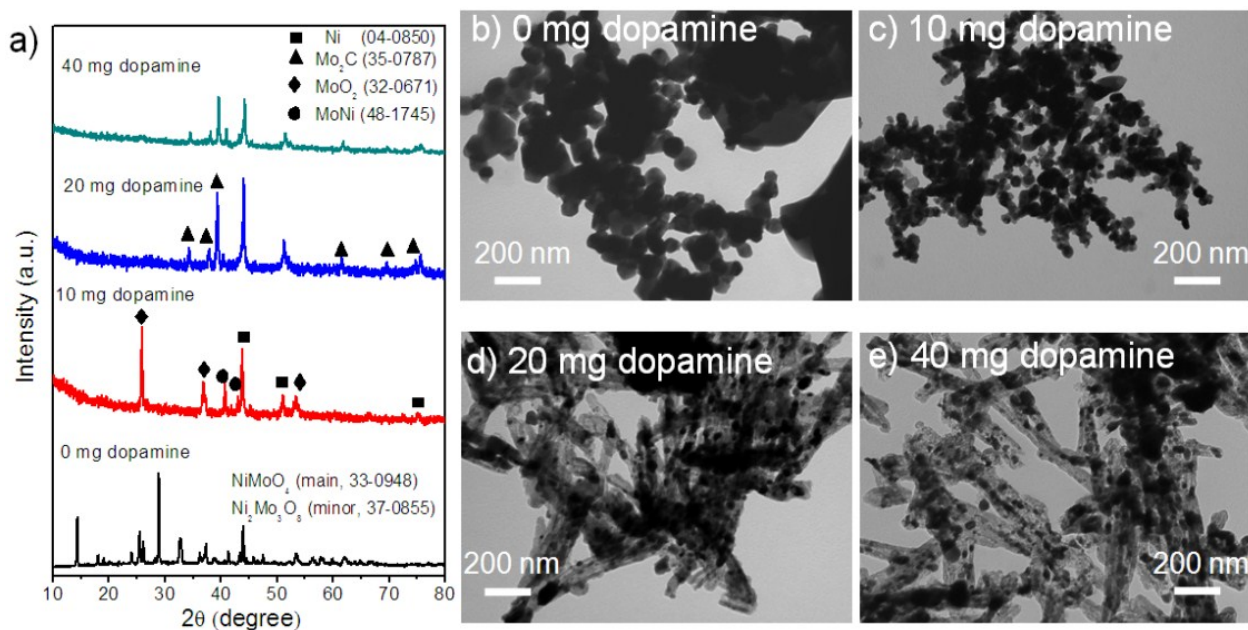


Fig. S3 (a) XRD patterns of samples with different mass ratio of dopamine and NiMoO₄. TEM images of (b) 0 mg dopamine, (c) 10 mg dopamine, (d) 20 mg dopamine, and (e) 40 mg dopamine. Condition: keeping the temperature and the mass of NiMoO₄ constant (800 °C and 40 mg NiMoO₄).

Note: The XRD pattern of sample with 0 mg dopamine can be indexed to NiMoO₄ and Ni₂Mo₃O₈ phase. Increasing the dopamine mass to 10 mg, the XRD peaks can be indexed to MoO₂, Ni, and MoNi phase. Further improving the dopamine mass to 20 and 40 mg, the XRD peaks can be indexed to Mo₂C, Ni, and MoNi phase. After the dopamine mass reaches 60 mg, the phase can be totally converted to Mo₂C and Ni phase (Figure S2a). Therefore, the annealing process to obtain Ni/Mo₂C-PC catalyst can be speculated through the following reaction with the increasing carbon content:



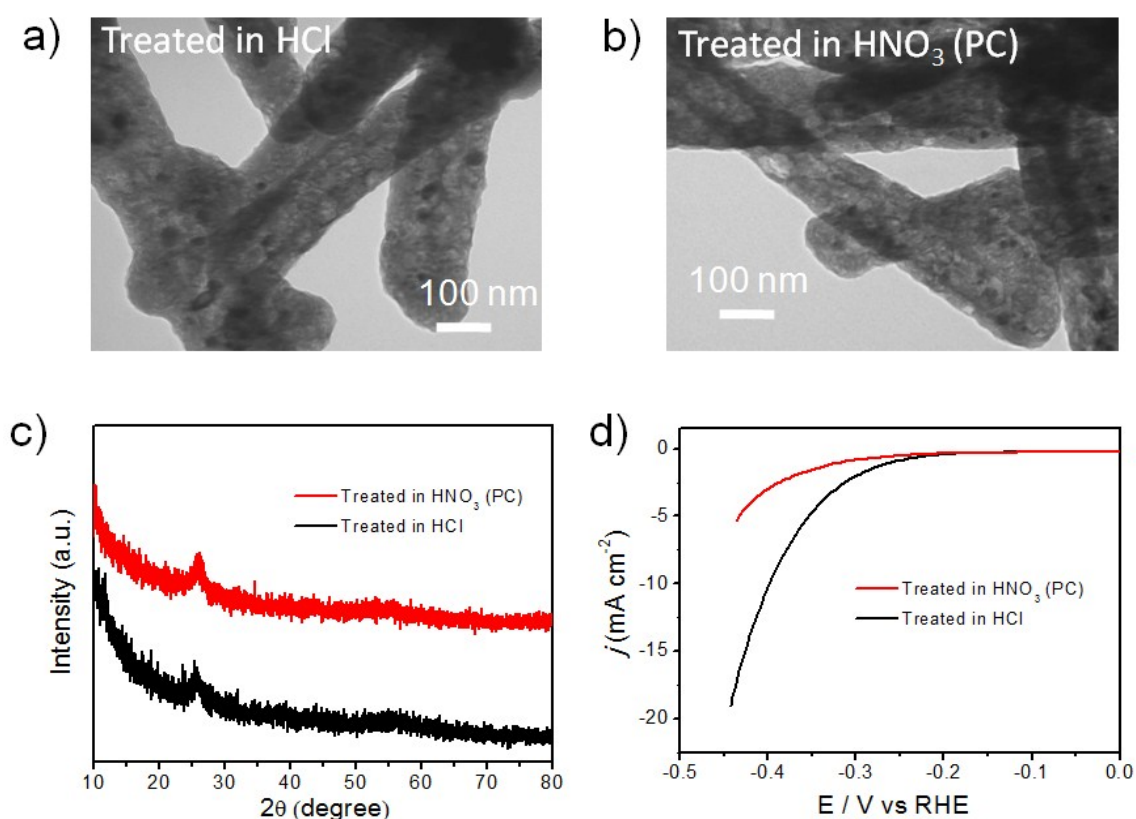


Fig. S4 (a) TEM image of Ni/Mo₂C-PC treated in 0.1 M HCl without heating. (b) TEM image of Ni/Mo₂C-PC treated in concentrated HNO₃ at 60 °C (PC). (c) XRD pattern and (d) HER test of these two samples.

Note: TEM images and XRD pattern revealed that most of Ni and Mo₂C nanoparticles were removed from the porous carbon. Based on the elemental mapping images, most of large Ni nanoparticles are surrounded by the small Mo₂C nanoparticles. It may be due to the small Mo₂C nanoparticle escaped from porous carbon after dissolving the large Ni nanoparticle support in the diluted HCl solution. The sample of Ni/Mo₂C-PC treated in HCl solution needed η of 398 mV to reach a current density of 10 mA cm⁻² for HER test, implying that most of active sites were removed. Meanwhile, the sample of Ni/Mo₂C-PC treated in HNO₃ solution cannot reach a current density of 10 mA cm⁻², which is consistent with the pure carbon materials or nitrogen-doped carbon materials.⁵⁻⁷ As a result, the sample of Ni/Mo₂C-PC treated in HNO₃ solution was used as the control sample of porous carbon (PC).

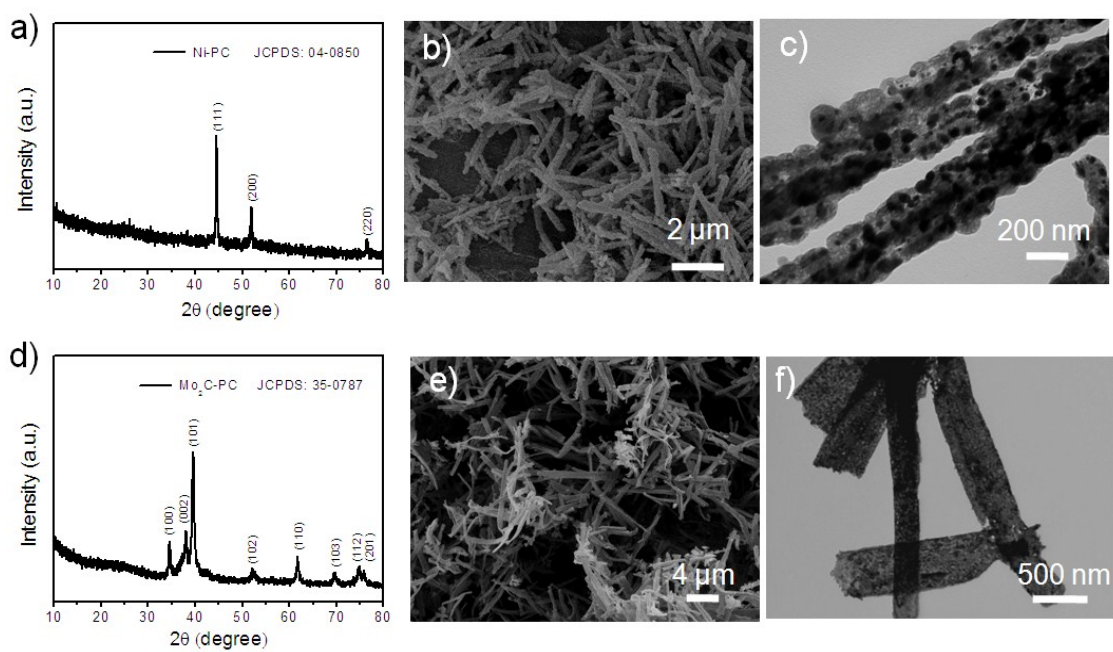


Fig. S5 (a) XRD pattern, (b) SEM and (c) TEM images of Ni-PC. (d) XRD pattern, (e) SEM and (f) TEM images of Mo₂C-PC.

Note: According to the ICP results, the weight percent of Ni in the Ni-PC is 47.6 wt% and Mo₂C in the Mo₂C-PC is 52.7 wt%, which are close to the sum 50.6 wt% of Ni and Mo₂C in the Ni/Mo₂C-PC (20.9 wt% for Ni and 29.7 wt% for Mo₂C).

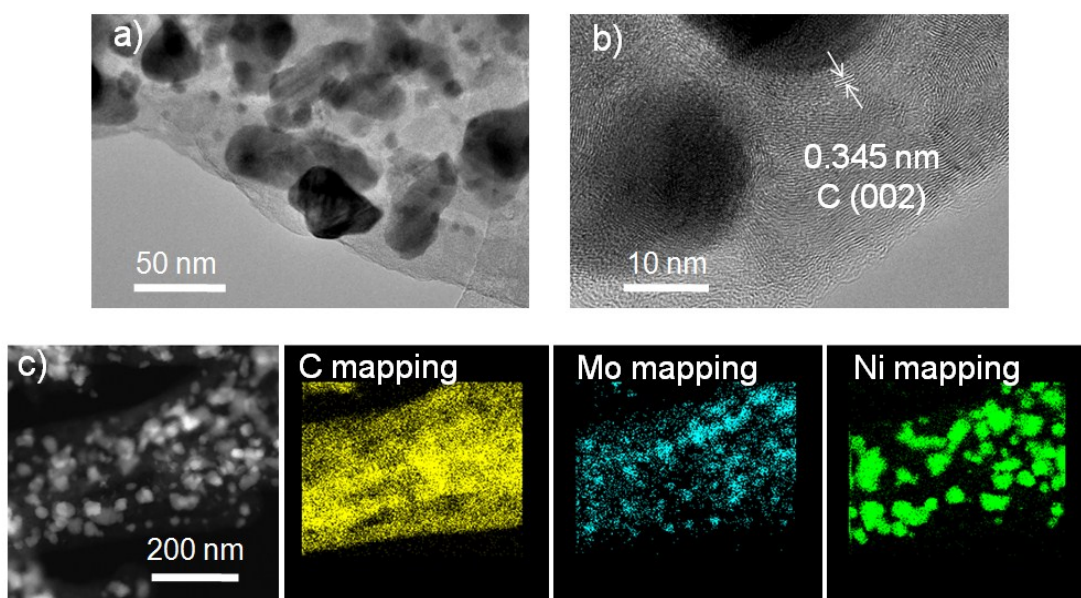


Fig. S6 (a) High magnification TEM images of Ni/Mo₂C-PC. (b) HRTEM image of carbon. (c) EDX elemental mapping images of C, Mo, and Ni.

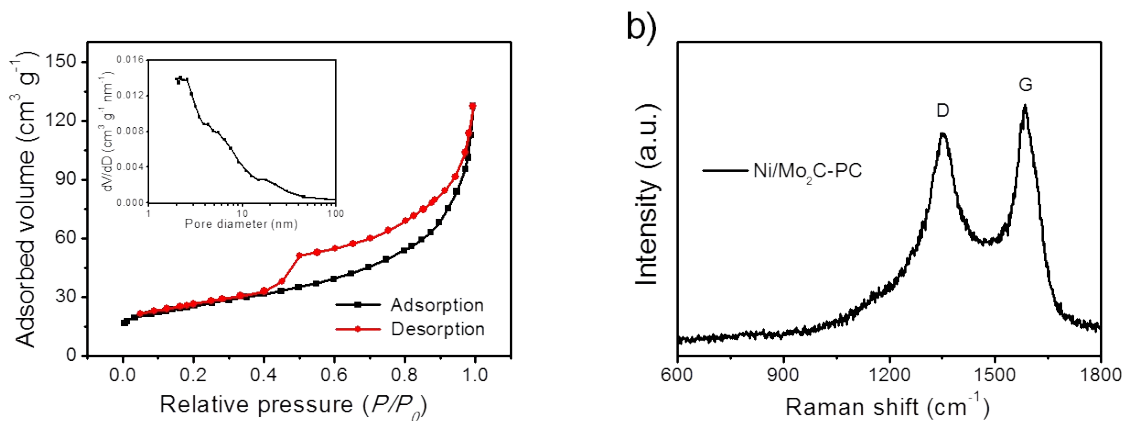


Fig. S7 (a) Nitrogen adsorption-desorption isotherm of Ni/Mo₂C-PC. The inset is the pore size distribution. (b) Raman spectrum of Ni/Mo₂C-PC.

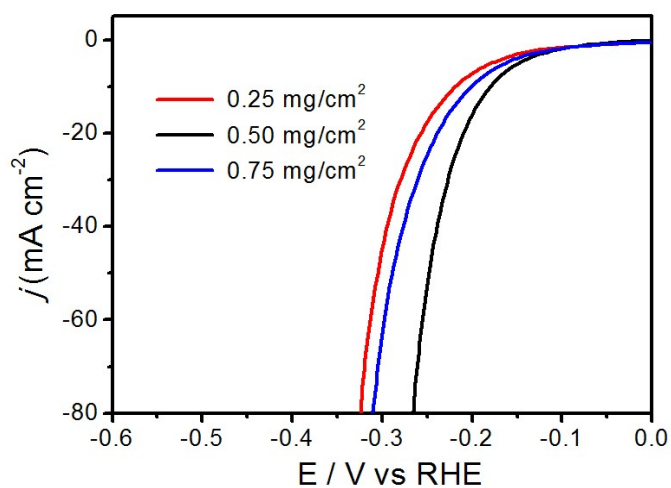


Fig. S8 Electrocatalytic study for HER. HER polarization curves of Ni/Mo₂C-PC catalyst at different mass loading on GC electrode, suggesting that the optimized mass loading is 0.50 mg cm⁻².

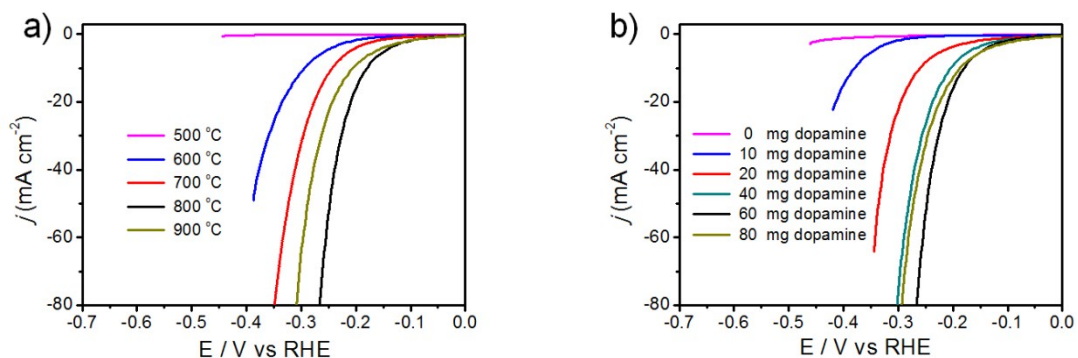


Fig. S9 Electrocatalytic study for HER. (a) HER polarization plots of NiMoO₄@PDA samples treated at 500-900 °C. Condition: 40 mg NiMoO₄ and 60 mg dopamine. (b) HER polarization plots of different mass of dopamine. Condition: 40 mg NiMoO₄ and 800 °C. The loading of all catalysts is 0.50 mg cm⁻² supported on GC electrode.

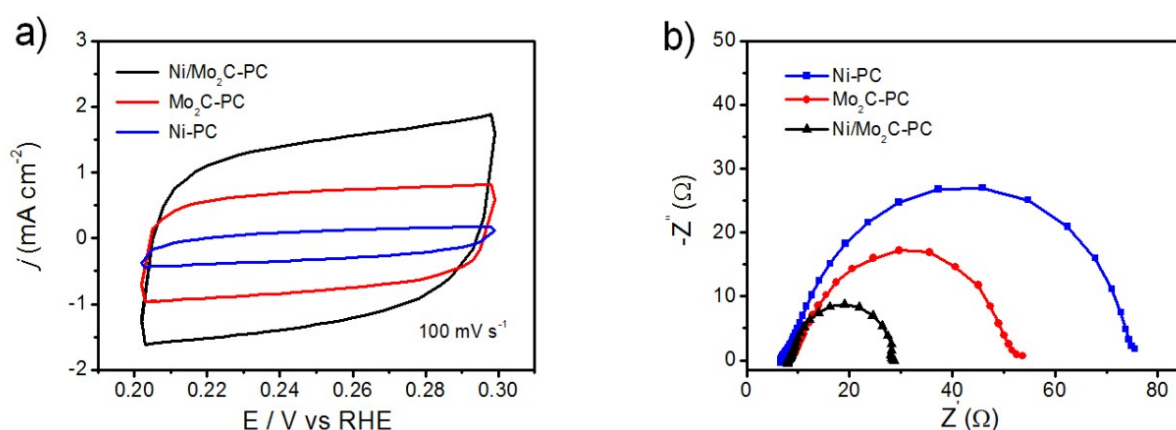


Fig. S10 Electrocatalytic study for HER. (a) The typical CV curves for Ni/Mo₂C-PC, Mo₂C-PC, Ni-PC at a scan rate of 100 mV s⁻¹ within a potential of 0.2-0.3 V (vs. RHE) for electrochemical surface area (ECSA) tests. (b) EIS Nyquist plots for different catalysts with η of 245 mV. The loading of all catalysts is 0.50 mg cm⁻² supported on GC electrode.

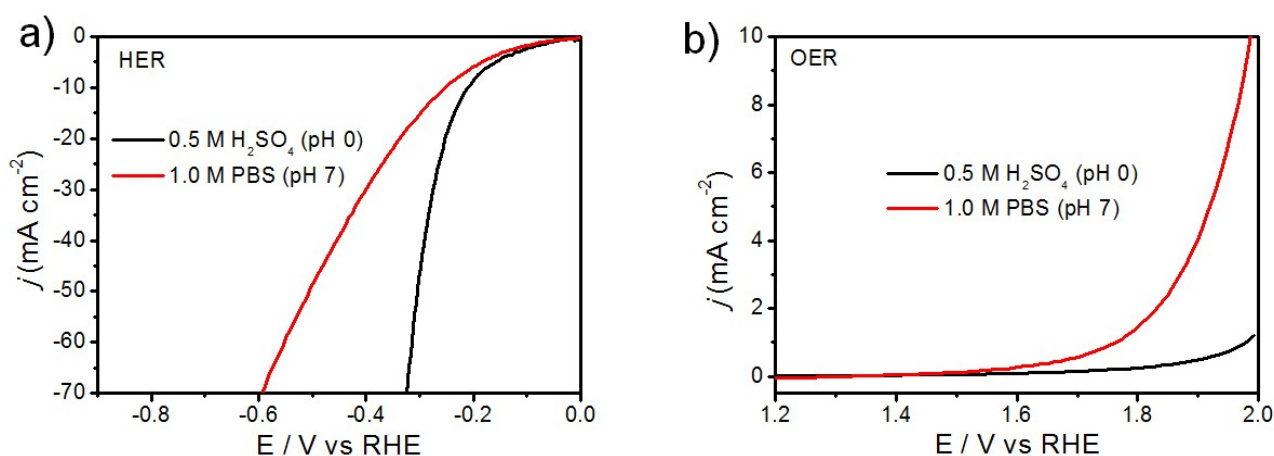


Fig. S11 Electrocatalytic study of Ni/Mo₂C-PC in acidic and neutral electrolytes. (a) HER and (b) OER polarization plots. The loading of catalyst is 0.50 mg cm⁻² supported on GC electrode.

Note: Our Ni/Mo₂C-PC materials catalyzed HER efficiently in acidic and neutral electrolytes, which needed low overpotentials of 210 and 250 mV to achieve a current density of 10 mA cm⁻², respectively. However, our catalyst exhibited poor performances for OER in acidic and neutral electrolytes, which was much worse than that in alkaline electrolyte. These results are consistent with most reported non-noble metal catalysts that HER can be catalyzed at wide pH values while OER only at alkaline media.

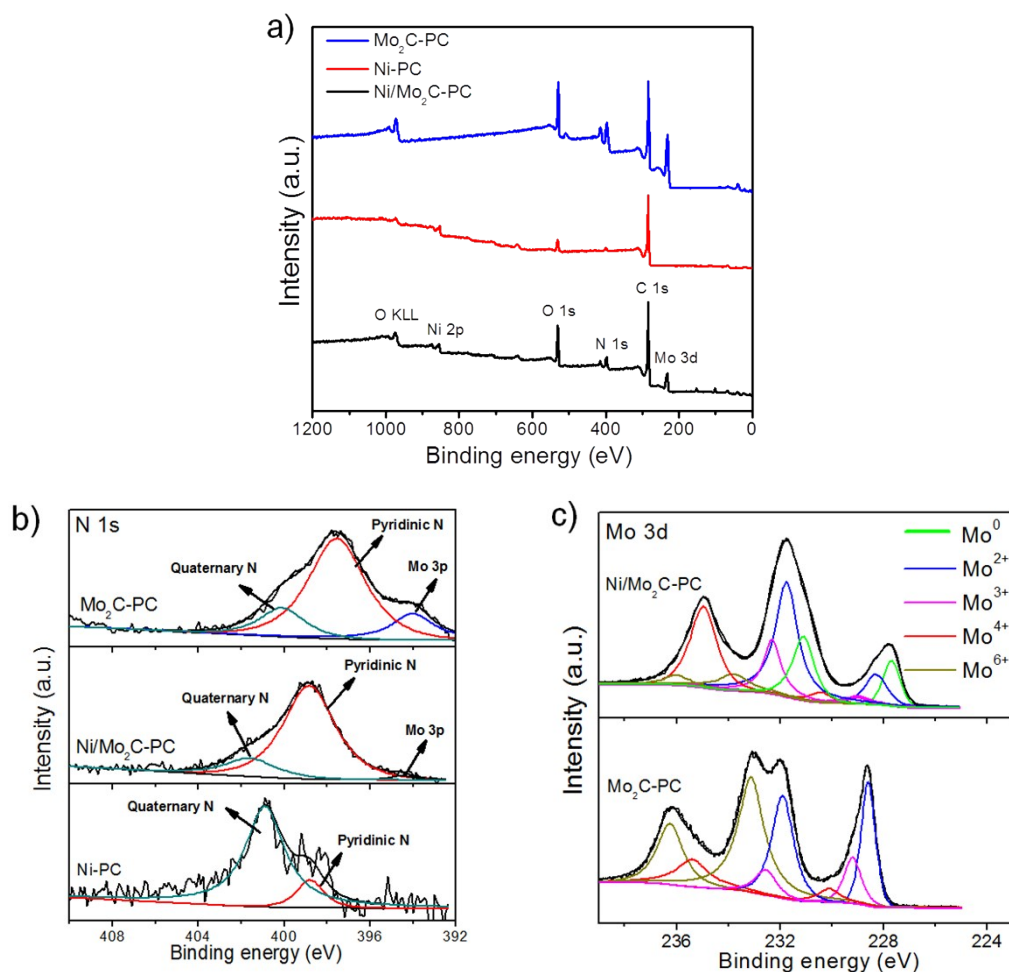


Fig. S12 (a) Overview XPS spectra. (b) High-resolution N 1s XPS spectra. (c) High-resolution Mo 3d XPS spectra.

Note: The XPS results give the N content of 8.4 at%, 15.8 at%, and 5.0 at% for Ni/Mo₂C-PC, Mo₂C-PC, and Ni-PC, respectively. Although Mo₂C-PC has the highest N content, the catalytic activity of Mo₂C-PC is obviously lower than that of Ni/Mo₂C-PC. Thus, it can be reasonably inferred that the N dopant is not the main reason for the enhanced activity of Ni/Mo₂C-PC.

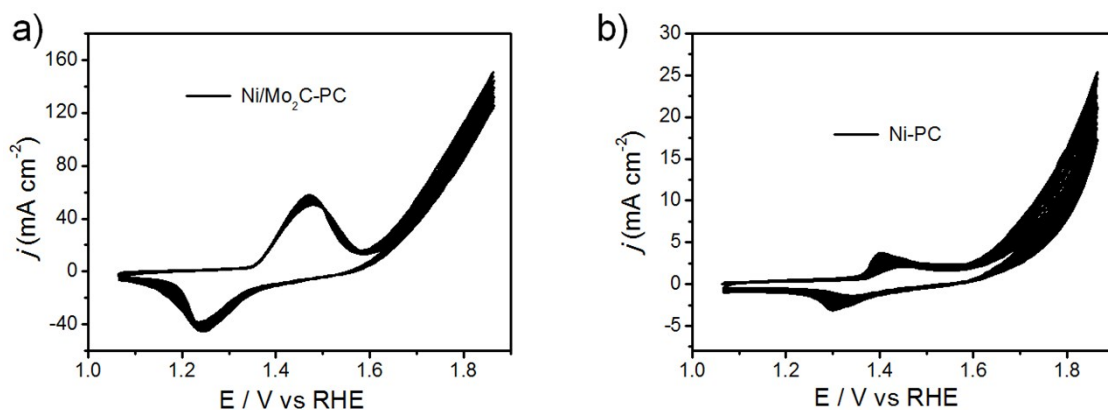


Fig. S13 OER cyclic tests of (a) Ni/Mo₂C-PC and (b) Ni-PC catalysts at a scan rate of 100 mV s⁻¹ for 20 cycles. The loading of catalyst is 0.50 mg cm⁻² supported on GC electrode. The curves here were without iR compensated.

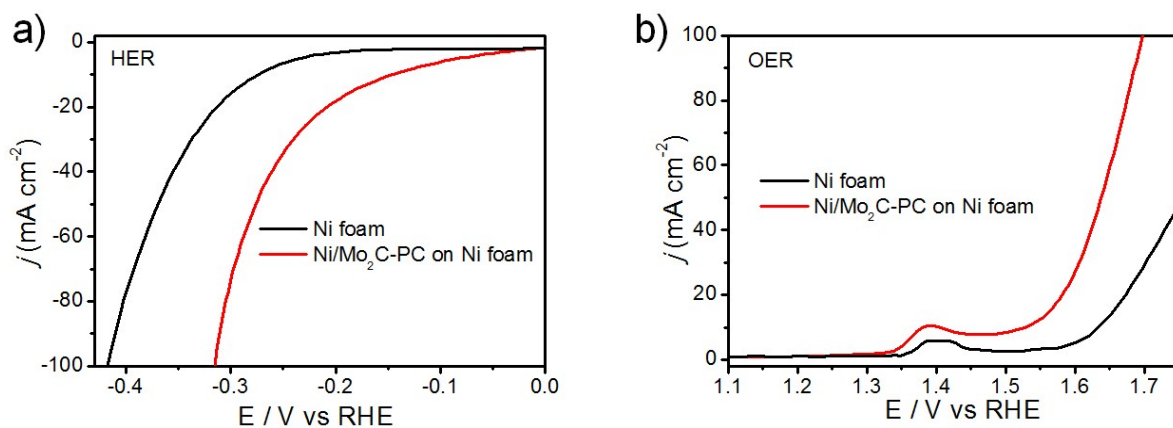


Fig. S14 (a) HER and (b) OER polarization plots of Ni/Mo₂C-PC catalyst with a loading of 2 mg cm⁻² supported on Ni foam electrode.

Note: Ni/Mo₂C-PC catalyst supported on Ni foam needs η of 145 mV for HER and 297 mV for OER to reach a current density of 10 mA cm⁻², which is obviously better than the bare Ni foam.

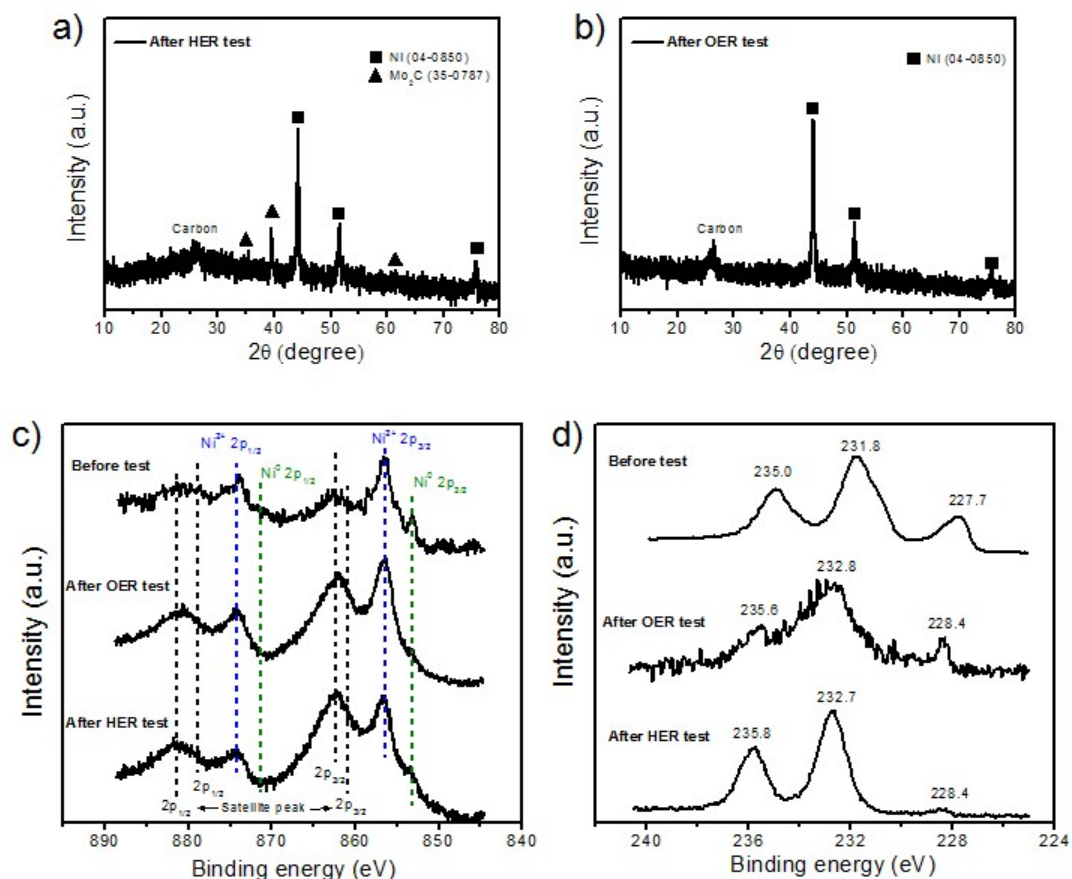


Fig. S15 XRD and XPS characterization of Ni/Mo₂C-PC catalyst after cyclic tests. (a) XRD pattern after HER test. (b) XRD pattern after OER test. (c) High-resolution Ni 2p XPS spectra. (d) High-resolution Mo 3d XPS spectra. The dissolved Mo after OER test can be reflected in the XRD pattern and the XPS result with strong baseline.

Note: Ni and Mo₂C phases can be detected for the sample after HER cyclic test. The Mo₂C phase disappeared when changing the cyclic test for OER. Mo₂C was oxidized to Mo⁶⁺ during the OER oxidation voltage, which was dissolved in alkaline electrolyte. However, the long-term stability test demonstrated that it can catalyze OER without any current loss but certain increase for 10 h (Fig. 5b), suggesting that Ni species may be the active site for OER. Based on Ni 2p XPS spectra, both HER and OER cyclic tests didn't change the valence state of Ni, showing the high stability of Ni²⁺ during the cyclic test. The Mo 3d peaks of samples after HER and OER cyclic tests shifted to the higher binding energy, suggesting the higher Mo valence after test.

Table S1. Comparison of the HER performance for Ni/Mo₂C-PC catalyst with other reported catalysts in basic electrolytes (1 M NaOH or 1 M KOH).

| Catalyst | Loading density (mg/cm ²) | Onset potential (mV vs. RHE) ^[a] | η at $j = 10 \text{ mA/cm}^2$ (mV) | Reference |
|-------------------------|---------------------------------------|---|---|---------------------------------------|
| NiO/Ni-CNT | 0.28 | <i>ca.</i> -20 | 80 | Nat. Commun. 2014, 5, 4695 |
| MoC _x | 0.8 | -80 | 151 | Nat. Commun. 2015, 6, 6512 |
| CoP nanowire array | 0.92 | -80 | 209 | J. Am. Chem. Soc. 2014, 136, 7587. |
| NiFe LDH/NF | N/A | <i>ca.</i> -75 | 210 | Science 2014, 345, 1593 |
| MoB | 2.3 | -140 | ~220 | Angew. Chem. Int. Ed. 2012, 51, 12703 |
| CoO _x @CN | 0.12 | -85 | 232 | J. Am. Chem. Soc. 2015, 137, 2688 |
| Ni(OH) ₂ /NF | N/A | <i>ca.</i> -120 | 250 | Science 2014, 345, 1593 |
| Mo ₂ C-NCNT | 3 | -72 | 257 | J. Mater. Chem. A, 2015, 3, 5783 |
| Mo ₂ C | 0.009 | <i>ca.</i> -140 | 270 | J. Am. Chem. Soc. 2015, 137, 7035 |
| WN nanorod array | 2.5 | <i>ca.</i> -200 | 285 | Electrochim. Acta, 2015, 154, 345. |
| Co-NRCNTs | ~0.28 | -100 | 370 | Angew. Chem. Int. Ed. 2014, 53, 4372 |
| Co-P/Co-PO ₄ | 0.1 | <i>ca.</i> -250 | ~380 | Adv. Mater. 2015, 27, 3175 |
| Ni/Mo ₂ C-PC | 0.50 | -60 | 179 | This work |

[a] It should be noted that we defined the potential at a HER current density of 1 mA cm⁻² as the onset potential.⁴

Table S2. Comparison of the OER performance for Ni/Mo₂C-PC catalyst with other reported catalysts in basic electrolytes (1 M NaOH or 1 M KOH).

| Catalyst | Loading density (mg/cm ²) | Onset potential (V vs. RHE) ^[a] | η at $j = 10 \text{ mA/cm}^2$ (mV) | Reference |
|---------------------------------------|---------------------------------------|--|---|-------------------------------------|
| NiFe-LDH/CNT | 0.2 | 1.45 | 247 | J. Am. Chem. Soc. 2013, 135, 8452 |
| NiCo LDH | 0.17 | 1.53 | 367 | Nano Lett. 2015, 15, 1421 |
| Bulk NiFe LDH | 0.07 | ~1.52 | 347 | Nat. Commun. 2014, 5, 4477 |
| Exfoliated NiFe LDH | 0.07 | ~1.48 | 302 | Nat. Commun. 2014, 5, 4477 |
| Bulk NiCo LDH | 0.07 | ~1.54 | 385 | Nat. Commun. 2014, 5, 4477 |
| Exfoliated NiCo LDH | 0.07 | ~1.52 | 334 | Nat. Commun. 2014, 5, 4477 |
| NiCo _{2.7} (OH) _x | 0.2 | 1.48 | 350 | Adv. Energy Mater. 2015, 5, 1401880 |
| NiCo(OH) _x | 0.2 | 1.50 | 410 | Adv. Energy Mater. 2015, 5, 1401880 |
| NiO _x | N/A | ~1.58 | 420 | J. Am. Chem. Soc. 2013, 135, 16977 |
| NiCuO _x | N/A | ~1.55 | 410 | J. Am. Chem. Soc. 2013, 135, 16977 |
| NiCoO _x | N/A | ~1.55 | 380 | J. Am. Chem. Soc. 2013, 135, 16977 |
| NiFeO _x | N/A | ~1.53 | 350 | J. Am. Chem. Soc. 2013, 135, 16977 |
| IrO _x | N/A | ~1.45 | 320 | J. Am. Chem. Soc. 2013, 135, 16977 |
| Ni/Mo ₂ C-PC | 0.50 | 1.50 | 368 | This work |

[a] It should be noted that we defined the potential at a OER current density of 1 mA cm⁻² as the onset potential.⁴

Table S3. Comparison of the bifunctional water-splitting activity of Ni/Mo₂C-PC catalyst with other reported bifunctional catalysts in basic electrolytes (1 M NaOH or 1 M KOH).

| Catalyst | Loading density (mg/cm ²) | Current density j | Voltage at the corresponding j | Reference |
|------------------------------------|---------------------------------------|-----------------------|--------------------------------|---------------------------------------|
| Pristine NiFeO _x /CFP | 1.6 | 10 mA/cm ² | ~1.88 V | Nat. Commun. 2015, 6, 7261 |
| 2-cycle NiFeO _x /CFP | 1.6 | 10 mA/cm ² | 1.61 V | Nat. Commun. 2015, 6, 7261 |
| NiSe/NF | 2.8 | 10 mA/cm ² | 1.63 V | Angew. Chem. Int. Ed. 2015, 54, 9351 |
| Ni ₅ P ₄ /NF | 3.5 | 10 mA/cm ² | 1.69 V | Angew. Chem. Int. Ed. 2015, 54, 12361 |
| CoP _x /NC | 1.0 | 10 mA/cm ² | ~ 1.71 V | Chem. Mater. 2015, 27, 7636 |
| NiFe LDH/NF | N/A | 10 mA/cm ² | 1.70 V | Science 2014, 345, 1593 |
| 3.5 nm Pt /NF | N/A | 10 mA/cm ² | 1.71 V | Science 2014, 345, 1593 |
| Ni(OH) ₂ /NF | N/A | 10 mA/cm ² | 1.82 V | Science 2014, 345, 1593 |
| Ni ₃ S ₂ /NF | 1.6 | 13 mA/cm ² | 1.76 V | J. Am. Chem. Soc. 2015, 137, 14023 |
| Ni/Mo ₂ C-PC/NF | 2.0 | 10 mA/cm ² | 1.66 V | This work |

References

1. Y. Ding, Y. Wan, Y.-L. Min, W. Zhang and S.-H. Yu, *Inorg. Chem.*, 2008, **47**, 7813-7823.
2. F. Jiang, W. Li, R. Zou, Q. Liu, K. Xu, L. An and J. Hu, *Nano Energy*, 2014, **7**, 72-79.
3. B. Liu, H. Yang, H. Zhao, L. An, L. Zhang, R. Shi, L. Wang, L. Bao and Y. Chen, *Sens. Actuators, B*, 2011, **156**, 251-262.
4. X. Zou and Y. Zhang, *Chem. Soc. Rev.*, 2015, **44**, 5148-5180.
5. X. Zou, X. Huang, A. Goswami, R. Silva, B. R. Sathe, E. Mikmeková and T. Asefa, *Angew. Chem. Int. Ed.*, 2014, **53**, 4372-4376.
6. Y. Zheng, Y. Jiao, Y. Zhu, L. H. Li, Y. Han, Y. Chen, A. Du, M. Jaroniec and S. Z. Qiao, *Nat. Commun.*, 2014, **5**, 3783.
7. Y. Ito, W. Cong, T. Fujita, Z. Tang and M. Chen, *Angew. Chem. Int. Ed.*, 2015, **54**, 2131-2136.